NOVEMBER 01 1999

Sound propagation over concave surfaces

Qiang Wang; Kai Ming Li

J. Acoust. Soc. Am. 106, 2358–2366 (1999)
https://doi.org/10.1121/1.428073

Sound propagation over concave surfaces

Qiang Wang
Department of Environmental & Mechanical Engineering, Faculty of Technology, The Open University, Milton Keynes MK 7 6AA, United Kingdom

Kai Ming Li[a)]
Department of Mechanical Engineering, Hong Kong Polytechnic University, Hung Hom, Kowloon, Hong Kong

(Received 11 December 1997; revised 1 July 1999; accepted 26 July 1999)

Diffraction of sound by concave surfaces is investigated theoretically and experimentally. In an earlier study [J. Acoust. Soc. Am. **104**, 2683–2691 (1998)], it has been demonstrated that a rigorous analogy exists for the sound field above a convex circular cylinder in an otherwise homogeneous medium. The predicted sound field corresponds to the situation where the sound speed of the medium decreases exponentially with height. Extending the previous work, this paper investigates of the sound field above a concave surface and explores the corresponding analogy. Normal mode solutions have been developed for a downward refracting medium with an exponential sound speed profile. The solutions are used to predict the sound fields diffracted by a cylindrical concave surface. A series of laboratory experiments is conducted using point monopole, horizontal dipole, and vertical dipole sources over cylindrical concave surfaces. The experimental measurements are compared with the normal mode predictions. For monopole and horizontal dipole sources, good agreement has been found between measurements and the normal mode predictions using an exponential profile. However, the agreement is less satisfactory where the sound field was due to vertical dipole sources. © *1999 Acoustical Society of America.* [S0001-4966(99)05411-9]

PACS numbers: 43.20.Fn, 43.28.Fp [LCS]

INTRODUCTION

Diffraction of waves by convex surfaces is of interest in many fields. It has been studied in great detail since the initial work of Fock[1] for the propagation of electromagnetic waves and subsequent work in acoustics by Pierce[2] and others.[3–5] In more recent studies, Chambers *et al.*[6] have used the fast field formulation to reexamine the sound field above a convex circular cylinder. On the other hand, Li *et al.*[7] have used the residue series approach to explore the 3-D sound fields above convex impedance surfaces. However, there is relatively little attention focused on the diffraction of sound by concave surfaces and most of these earlier studies have been concerned with monopole sources. Two notable exceptions are, first, a study by Almgren[8] where he measured the sound field above a rigid concave curved surface. He reported that the measurements agreed reasonably well with the sound fields calculated by using the theories of Pridmore-Brown,[9,10] Pierce,[3] and Rasmussen[11] for propagation over a flat rigid ground in a downward refracting medium. He suggested that further work could be extended to a finite impedance surface. Second, Gabillet *et al.*[12] conducted analogous indoor experiments over rigid and finite impedance concave surfaces with the radius of curvature of 20 m. Satisfactory agreements were obtained for a receiver locating at a few wavelengths above the curved surface. We remark that these two previous studies were aimed to simulate the propagation of sound in a downward refracting medium.

In this paper, we report a continuation of our previous study[7] by examining the sound field above a concave surface both theoretically and experimentally. We consider not only monopole but also dipole sources. A normal mode solution is developed that is based on a recent study by Li and Wang.[13] Essentially, the residue series solution[7] for sound field above a convex cylindrical surface is extended to enable calculation of the sound field scattered by a concave cylindrical surface. Measurement results using point monopole and horizontal dipole and vertical dipole sources over cylindrical concave surfaces are reported and compared with theoretical predictions.

I. THE NORMAL MODE SOLUTION

It has been suggested[3] that an acoustic analogy exists between downwardly curving ray paths over flat ground and propagation over a concave surface in a neutral atmosphere. The analogy is illustrated in Fig. 1. Almgren[8] has shown that it is valid to use a concave surface to simulate the propagation of sound in the downward refracting atmosphere. The corresponding sound speed profile is modeled in a bilinear form where the speed of sound, $c(z)$, is expressed in terms of the vertical height, z ($z \ll R_c$), as

$$c(z) = \frac{c_0}{\sqrt{1-2z/R_c}} \approx c_0\left(1+\frac{z}{R_c}-\frac{2z^2}{3R_c^2}+\cdots\right). \tag{1}$$

In Eq. (1), $c_0 \equiv c(0)$, and R_c is the radius of the curved surface. We note that, to first approximation, $1/R_c \approx (dc/dz)/c_0$ may be interpreted as the normalized sound speed gradient for the downward refracting atmosphere. Given the bilinear sound speed profile, the normal mode so-

a)Electronic mail: mmkmli@polyu.edu.hk

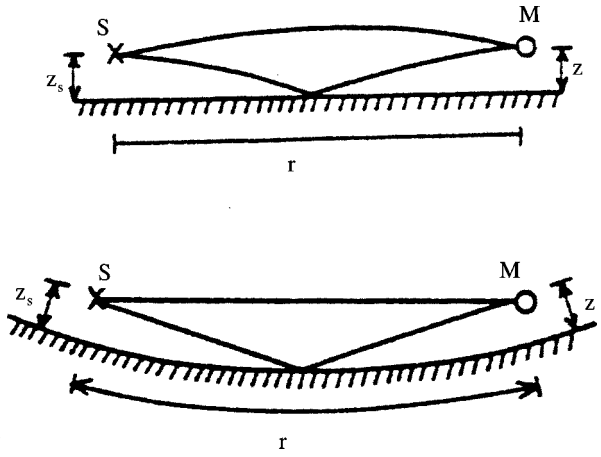

FIG. 1. Sketch showing the analogy between curved ray path above a plane boundary and straight-line propagation above a concave surface.

lution for the sound field, $p(r,z)$, can be expressed in terms of Airy functions Ai and their derivatives Ai′ as[13,14]

$$p^{(b)}(r,z) = \frac{i\pi e^{-i\pi/4}}{l}\sum_n \sqrt{\frac{2}{\pi K_n r}}\,\frac{\mathrm{Ai}(\tau_n + z_s/l)\mathrm{Ai}(\tau_n + z/l)e^{iK_n r}}{\{\tau_n[\mathrm{Ai}(\tau_n)]^2 - [\mathrm{Ai}'(\tau_n)]^2\}}, \tag{2}$$

where

$$\tau_n = (K_n^2 - k_0^2)l^2 \quad \text{for } n = 0,1,2,3,\ldots. \tag{3}$$

The variables τ_n (for $n=0,1,2,3,...$) are the zeros of the dispersion equation:

$$\mathrm{Ai}'(\tau_n) + q_n \mathrm{Ai}(\tau_n) = 0, \tag{4}$$

with

$$q_n = ik_0\beta l_n, \tag{5a}$$

$$l_n = (R_c/2k_0^2)^{1/3} = l, \tag{5b}$$

say, $k_0(\equiv 2\pi f/c_0)$ is the reference wave number, r is the distance from the source along the curved surface, z_s and z are, respectively, the source and receiver heights, and K_n is the horizontal wave number of the nth mode. In Eq. (2), the superscript (b) denotes the sound field in a medium with the bilinear sound speed profile. Here, in Eqs. (4) and (5a), q_n may be regarded as the nondimensional scaled admittance,[15] l_n as the wave layer thickness,[14] and β as the specific normalized admittance of the ground. It is evident from Eqs. (5a) and (5b) that the wave layer thickness and the nondimensional scaled admittance are the same for all modes for the case of the bilinear profile.

With the acoustic analogy suggested by Refs. 3 and 8, it is possible to use Eq. (2) to approximate the sound field above a concave cylindrical surface in an otherwise homogeneous medium. However, Di and Gilbert[16] suggest a stricter acoustic analogy by using a conformal transformation. They show that an exponential sound speed profile should be used instead of the bilinear profile in predicting the sound field. In this paper, we wish to investigate the validity of approximating the sound field above a concave cylindrical surface in a homogeneous medium by using the bilinear sound speed profile over a flat surface.

Using the same approach, Li *et al.*[7] extend the conformal transformation to three dimensions and they derive a residue series solution for the sound field behind a long convex cylinder. In the light of these earlier studies, it is possible to show that the sound field scattered by a concave cylindrical surface in a homogenous medium is identical to the sound field above an impedance flat ground surface in the presence of an exponential sound speed profile.[17] In the downward refracting medium, the speed of sound is determined according to

$$c(z) = c_0 \exp(z/R_c) \approx c_0\left(1 + \frac{z}{R_c} + \frac{z^2}{2R_c^2} + \cdots\right), \tag{6}$$

where $z \ll R_c$. Making use of our previous analyses,[7,13] we can show that the sound field above a concave cylinder is given by

$$p^{(c)}(r,\psi_r,z) = e^{i\pi/4}\sqrt{\frac{8\pi}{r}}\sum_n \left[\frac{\bar{\xi}_s\bar{\xi}}{\bar{k}_z^2(z_s)\bar{k}_z^2(z)}\right]^{1/4} \frac{\sqrt{K_n}\mathrm{Ai}(-\bar{\xi}_s)\mathrm{Ai}(-\bar{\xi})e^{iK_n r}}{(\partial\tau_n/\partial K_n)\{\tau_n[\mathrm{Ai}(\tau_n)]^2 - [\mathrm{Ai}'(\tau_n)]^2\} + (\partial q_n/\partial K_n)[\mathrm{Ai}(\tau_n)]^2}, \tag{7}$$

where

$$\bar{\xi}(z) = \begin{cases} \left\{\frac{3}{2}K_n R_c \cos\psi_r\left[\frac{\bar{k}_z(z)}{K_n\cos\psi_r} - \tan^{-1}\left(\frac{\bar{k}_z(z)}{K_n\cos\psi_r}\right)\right]\right\}^{2/3} & \text{if } z \leqslant \mathrm{Re}(z_t), \\ -\left\{\frac{3}{2}K_n R_c \cos\psi_r\left[-\frac{\sqrt{-\bar{k}_z^2(z)}}{K_n\cos\psi_r} + \tanh^{-1}\left(\frac{\sqrt{-\bar{k}_z^2(z)}}{K_n\cos\psi_r}\right)\right]\right\}^{2/3} & \text{if } z > \mathrm{Re}(z_t), \end{cases} \tag{8}$$

$$z_t = R_c \ln\left(\frac{\sqrt{k_0^2 - K_n^2\sin^2\psi_r}}{K_n\cos\psi_r}\right), \tag{9}$$

$$\bar{k}_z(z) = +\sqrt{(k_0^2 - K_n^2\sin^2\psi_r)\exp(-2z/R_c) - K_n^2\cos^2\psi_r}, \tag{10}$$

ψ_r is the azimuthal angle of the receiver in the plane of constant z, the superscript (c) denotes the sound field above a cylindrical concave surface, and z_t is known as the turning point[13] in the terminology of ray acoustics. Again, the variable τ_n represents the zeros of Eq. (4) but it is expressed, in terms of K_n, differently as follows:

$$\tau_n = -\xi(0) = -\left\{\frac{3}{2}K_n R_c \cos\psi_r \times\left[\frac{\sqrt{k_0^2-K_n^2}}{K_n\cos\psi_r}-\tan^{-1}\left(\frac{\sqrt{k_0^2-K_n^2}}{K_n\cos\psi_r}\right)\right]\right\}^{2/3}. \tag{11}$$

In Eq. (5) the variable $\partial\tau_n/\partial K_n$ can be evaluated to give

$$\frac{\partial\tau_n}{\partial K_n} = \frac{R_c}{\sqrt{-\tau_n}}\sec\psi_r \tan^{-1}\left(\frac{\sqrt{k_0^2-K_n^2}}{K_n\cos\psi_r}\right). \tag{12}$$

The numerical values of τ_n, q_n, and K_n can be determined by using the method described in Refs. 7 and 13. Substituting these numerical values into Eq. (7), we can compute the sound field above a cylindrical curved surface. The numerical results for the bilinear and exponential sound speed profiles will be shown in Sec. II.

Noting that the horizontal range and the vertical-height-dependent factors are not coupled in the residue series solution for a monopole source, the dipole field p_d can be derived from the monopole field p by noting[18]

$$p_d = 2\Delta_d S_0\left[\sin\gamma_d\cos(\psi_d-\psi_r)\frac{\partial}{\partial r}p+\cos\gamma_d\frac{\partial}{\partial z_s}p\right], \tag{13}$$

where $2\Delta_d$ is the separation of the components of two out-of-phase monopole components and γ_d and ψ_d are the polar and azimuthal angles of the dipole moment vector.[6] The normal mode solution for a bilinear profile can be extended for an arbitrarily oriented dipole source over a concave surface, i.e.,

$$p_d^{(b)} = p_h^{(b)} + p_v^{(b)}, \tag{14}$$

where $p_h^{(b)}$ and $p_v^{(b)}$ are, respectively, the horizontal component and the vertical component of a dipole. They are determined according to[24]

$$p_h^{(b)}(r,\psi_r,z) \approx \frac{e^{i\pi/4}}{l}\sqrt{\frac{\pi}{2r^3}}S_d\sin\gamma_d\cos(\psi_d-\psi_r) \times\sum_n \frac{(2iK_n-1)\mathrm{Ai}(\tau_n+z_s/l)\mathrm{Ai}(\tau_n+z/l)e^{ik_n r}}{\sqrt{K_n}\{\tau_n[\mathrm{Ai}(\tau_n)]^2-[\mathrm{Ai}'(\tau_n)]^2\}}, \tag{15}$$

and

$$p_v^{(b)}(r,\psi_r,z) \approx \frac{\pi e^{i\pi/4}}{l^2}S_d\cos\gamma_d \times\sum_n \sqrt{\frac{2}{\pi K_n r}}\frac{\mathrm{Ai}'(\tau_n+z_s/l)\mathrm{Ai}(\tau_n+z/l)e^{iK_n r}}{\{\tau_n[\mathrm{Ai}(\tau_n)]^2-[\mathrm{Ai}'(\tau_n)]^2\}}. \tag{16}$$

The normal mode solution for an exponential profile for an arbitrarily oriented dipole source may be expressed by

$$p_d^{(c)} = p_h^{(c)} + p_v^{(c)}, \tag{17}$$

where

$$p_h^{(c)} \approx e^{i\pi/4}S_d\sin\gamma_d\cos(\psi_d-\psi_r) \times\sqrt{\frac{2\pi}{r^3}}\sum_n\left[\frac{\bar{\xi}_s\bar{\xi}}{\bar{k}_z^2(z_s)\bar{k}_z^2(z)}\right]^{1/4}\frac{(2iK_n-1)\sqrt{K_n}\mathrm{Ai}(-\bar{\xi}_s)\mathrm{Ai}(-\bar{\xi})e^{iK_n r}}{(\partial\tau_n/\partial K_n)\{\tau_n[\mathrm{Ai}(\tau_n)]^2-[\mathrm{Ai}'(\tau_n)]^2\}+(\partial q_n/\partial K_n)[\mathrm{Ai}(\tau_n)]^2}, \tag{18}$$

and

$$p_v^{(c)} \approx e^{i\pi/4}S_d\cos\gamma_d\sqrt{\frac{8\pi}{r}}\sum_n\left[\frac{\bar{k}_z^2(z_s)\bar{\xi}}{\bar{k}_z^2(z)\bar{\xi}_s}\right]^{1/4}\frac{\sqrt{K_n}\mathrm{Ai}'(-\bar{\xi}_s)\mathrm{Ai}(-\bar{\xi})e^{iK_n r}}{(\partial\tau_n/\partial K_n)\{\tau_n[\mathrm{Ai}(\tau_n)]^2-[\mathrm{Ai}'(\tau_n)]^2\}+(\partial q_n/\partial K_n)[\mathrm{Ai}(\tau_n)]^2}. \tag{19}$$

Locations of poles for dipole sources are the same as those for a monopole source and they are determined by solving the dispersion equation [see Eq. (4)].

II. THEORETICAL COMPARISONS

The normal mode solution for an exponential profile, Eq. (7), can be examined by means of numerical comparisons. A frequency of 2915 Hz corresponding to a wavelength of 0.12 m in atmosphere, at which some experiments have been conducted, is presented for these numerical comparisons.

A. Comparison of the normal mode solution to the fast field program results

The normal mode solution for an exponential profile should agree with the fast field program (FFP)[19] solution for

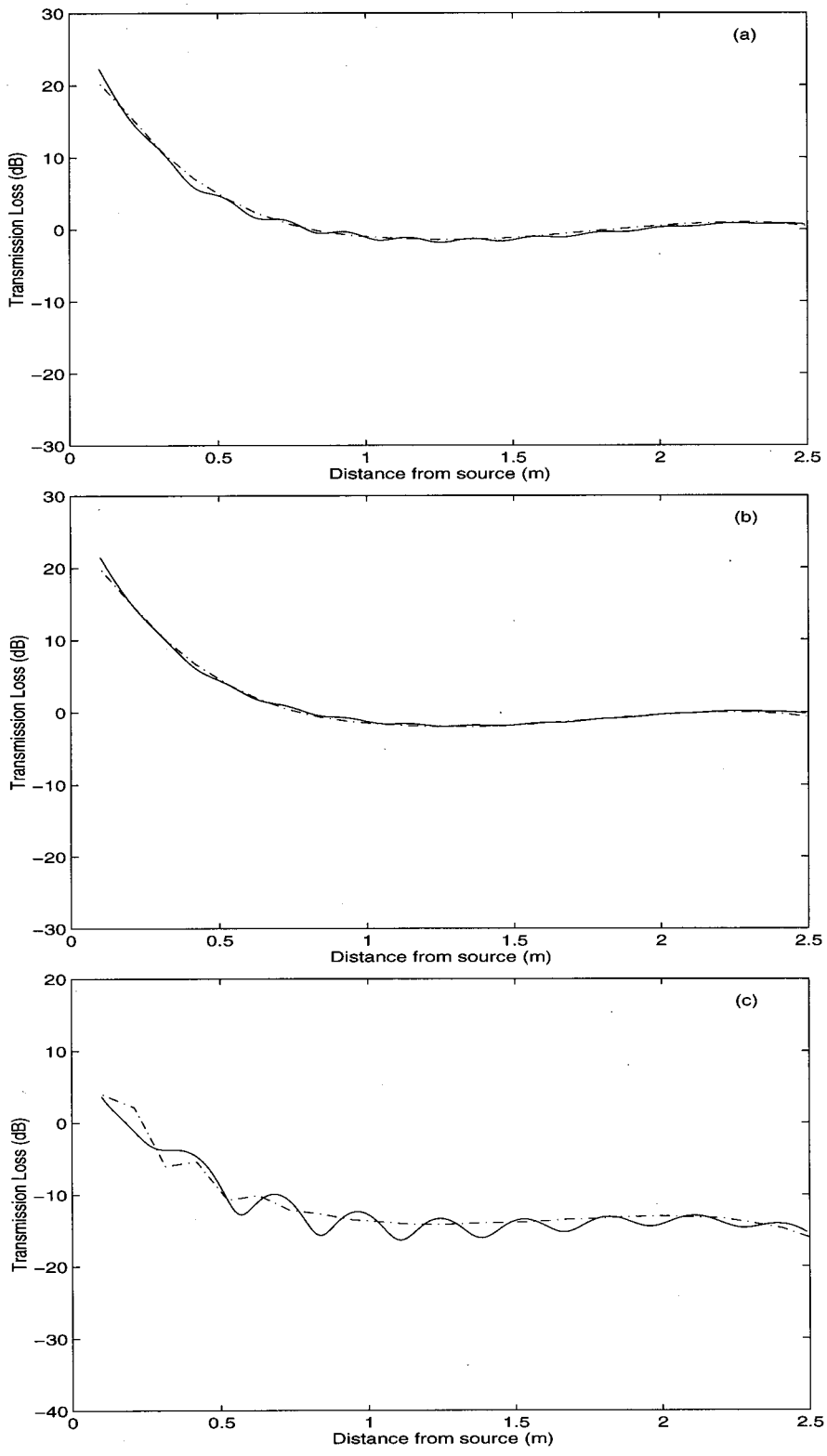

FIG. 2. Transmission loss predicted over a felt-covered concave surface with $R_c = 2.5$ m and $z_s = z = 0.10$ m at a frequency of 2915 Hz. Dash-dotted curves: FFP calculations, solid curves: the normal mode calculations with exponential profiles for (a) monopole, (b) horizontal dipole, and (c) vertical dipole.

the same sound speed gradient. To validate the numerical solutions, we compare the transmission loss (TL) versus the distance from source where

$$\mathrm{TL} = 20 \lg (p/p_1) \tag{20}$$

and p_1 is the free field acoustic pressure at a distance of 1 m from the source.

Figure 2 shows the results of the normal mode calculation (solid lines) compared with the FFP calculation (dash-dotted lines) for the sound speed profile varying exponentially with height. In Fig. 2(a), the sound propagation due to a monopole source above a felt-covered concave surface was predicted at a frequency of 2915 Hz with $R_c = 2.5$ m and the gradient was truncated at 1.24 m altitude. A good approxi-

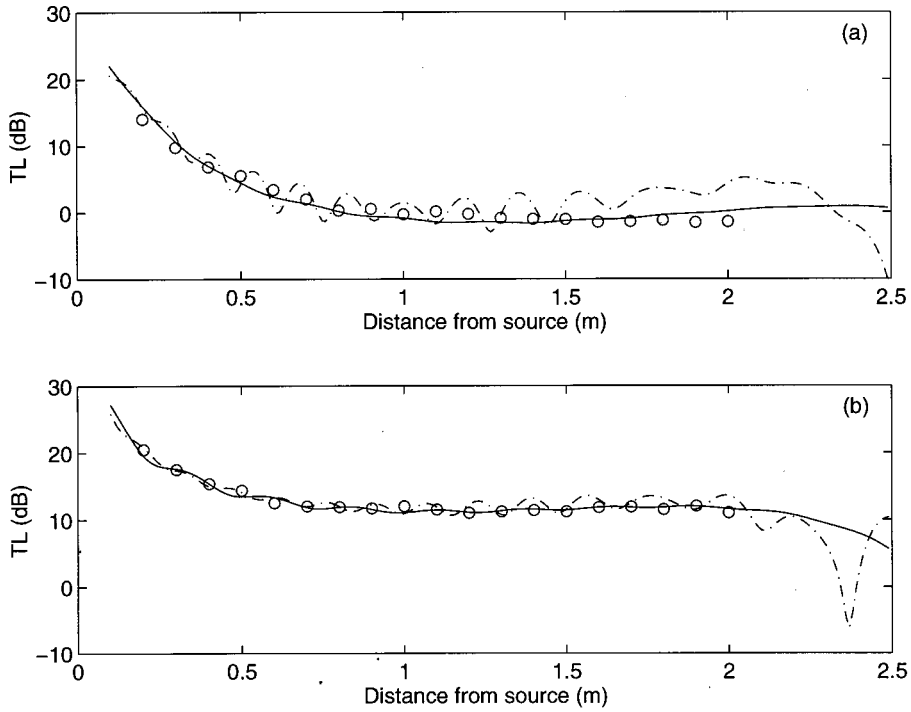

FIG. 3. Transmission loss due to a monopole source obtained at a frequency of 2915 Hz in a gradient with $R_c = 2.5$ m, over (a) a felt-covered concave surface with $z_s = z = 0.10$ m and (b) a rigid surface with $z_s = 0.02$ m and $z \sim 0.00$ m. Circles: measurements, solid curves: the normal mode calculations for exponential profiles, and dash-dotted curves: for bilinear profiles.

mation for the truncated gradient may be obtained by using 14 modes. This number of modes is the so-called full solution.[14] The complex impedance of the surface is calculated by using a two-parameter model[20] with $\sigma_e = 38\,\mathrm{kPa\,s\,m^{-2}}$ and $\alpha_e = 15\,\mathrm{m^{-1}}$. The chosen parameters (R_c, σ_e, and α_e) reflect the radius and the impedance of the curved surfaces used in our subsequent laboratory measurements. The source and receiver heights are 0.1 m. Figure 2(b) and (c) shows the comparisons for the propagation due to a horizontal dipole source and a vertical dipole source, respectively. The agreement between the two numerical schemes for monopole and horizontal dipole sources is excellent. However, for the vertical dipole source, the agreement between the FFP and the normal mode predictions is less satisfactory. There are considerable oscillations in the magnitudes of TL for the normal mode predictions. This is largely due to the fact that the contribution due to a branch-line integral has been ignored in the normal mode solution.[21] The inadequacy of the approximation is only apparent for the case of a vertical dipole because the solution involves the spatial differentiation with respect to the vertical height. In view of the acoustic analogy, the normal mode solution may be used to predict the sound field above a curved surface in an otherwise homogeneous medium. Its predictions will be compared with laboratory measurements in Sec. III.

B. Comparison of the normal mode solutions for two profiles

Typical comparisons of the normal mode predictions between bilinear and exponential profiles are displayed. Figure 3(a) shows the predictions above the felt-covered concave surface in a gradient with $R_c = 2.5$ m, at frequencies of 2915 Hz, for both profiles. The solid curves are calculated from Eq. (7) for the exponential sound speed profile and the dotted curves are calculated from Eq. (2) for the bilinear sound speed profile. The source height is 0.02 m and the receiver is on the surface. For the present situation, the wave layer thickness, l_n, and the wave number, k_0, can be determined as about 0.075 m and 54 $\mathrm{m^{-1}}$, respectively.

It is noteworthy that the predicted sound fields for the exponential and bilinear sound speed profiles are comparable only at ranges less than about 20 l_n. This feature is somewhat different from the case of upward refracting medium in which the predicted sound fields for both profiles are comparable in most practical situations.[7] However, this is not the case for the downward refracting medium. The difference becomes more significant when the receiver is located at a few wavelengths from the source. To illustrate the case, we consider the following example. A noise source of frequency 100 Hz is situated in a stratified medium with a normalized sound speed gradient of $1 \times 10^{-4}\,\mathrm{m^{-1}}$ (i.e., $R_c = 10\,000$ m). The wave layer thickness l_n can be determined as about 10 m. Hence, there should be notable discrepancies in the sound fields when the range extends beyond 200 m.

Over a rigid concave surface, the trends are similar to those over the felt-covered concave surface. The solid and dashed lines in Fig. 4(b) show the normal mode predictions for both profiles over a rigid surface with the source height of 0.02 m and the receiver on the surface.

C. Comparison with the boundary element method

To examine the calculations for both profiles over a cylindrical concave surface, the normal mode solutions are compared to the predictions due to the boundary element method (BEM). The BEM predictions serve an important purpose of ''benchmarking'' the normal mode solution because the numerical scheme of the BEM is based on an exact formulation of sound reflected by arbitrary surfaces. The numerical implementation of the BEM is well known and the details are described elsewhere.[22,23] In the BEM predictions,

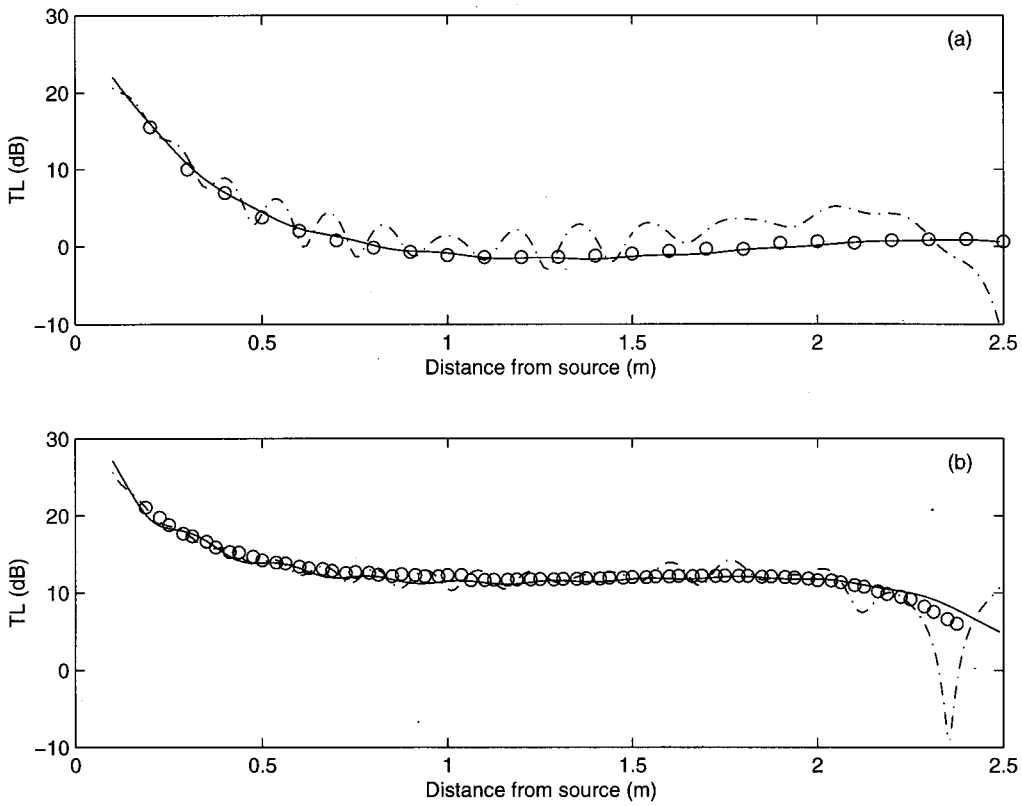

FIG. 4. Transmission loss predicted at a frequency of 2915 Hz in a gradient with $R_c = 2.5$ m, over (a) a felt-covered concave surface with $z_s = z = 0.10$ m and (b) a rigid surface with $z_s = 0.02$ m and $z \sim 0.00$ m. Circles: BEM calculations, solid curves: the normal mode calculations for exponential profiles, and dash-dotted curves: the normal mode calculations for bilinear profiles.

the cross section of the cylindrical concave surface is modeled as a series of adjacent elements with impedance surfaces.

Figure 4 shows two typical examples of prediction over concave surfaces, in a gradient with $R_c = 2.5$ m [(a) the felt-covered surface and (b) the rigid surface]. The solid lines represent the predictions for the exponential profile and the dotted lines represent those for the bilinear profile. The circles represent the calculations from the BEM.

There are considerable discrepancies between the normal mode predictions for the bilinear profile and predictions calculated from the BEM, especially at longer ranges. At short ranges, the discrepancies are small except that the normal mode solution shows considerable oscillations in magnitude. As the receiver is moved away from the source, the differences become greater.

Contrary to the bilinear sound speed profile, the normal mode predictions for the exponential profile accord generally with the BEM calculations over the concave surfaces. This implies that the equivalent sound speed increases exponentially rather than bilinearly with height over a cylindrical concave surface. This implication is in agreement with the conclusion obtained in the case of a cylindrical convex surface.[7] In the following section, the data obtained from measurements over cylindrical concave surfaces will be compared with the normal mode predictions for both sound speed profiles to test the performance of the theoretical models.

III. EXPERIMENTAL INVESTIGATIONS

A series of laboratory experiments was performed, using a point monopole source and horizontal and vertical dipole sources, above both felt-covered and rigid concave surfaces, to investigate sound propagation over concave surfaces. The experimental data is analyzed and compared to predictions of the normal mode solutions for both the exponential [Eq. (7)] and the bilinear [Eq. (2)] profiles.

A. Measurement techniques

The concave surfaces were constructed to behave either as rigid surfaces or as surfaces of finite impedance. The rigid concave surface was constructed by attaching sheets of masonite to a series of curved ribbed structures. The resulting surface was that of a long cylinder with a radius of curvature 2.5 m. It was built to have a transverse length of 2.5 m (subtended angle of about 60 degrees), a span of 1.8 m and a depth of 0.45 m. To ensure that the surface acted as a rigid reflector, particular care was paid in fastening the masonite sheets to the structures. To obtain a surface of finite impedance, felt was secured to the rigid surface using double-sided tape to eliminate the possible transmission path between the sheets and the felt. The impedance of the felt was characterized by measurements over a flat surface.[17] A two-parameter impedance model[20] with an effective flow resistivity of 38

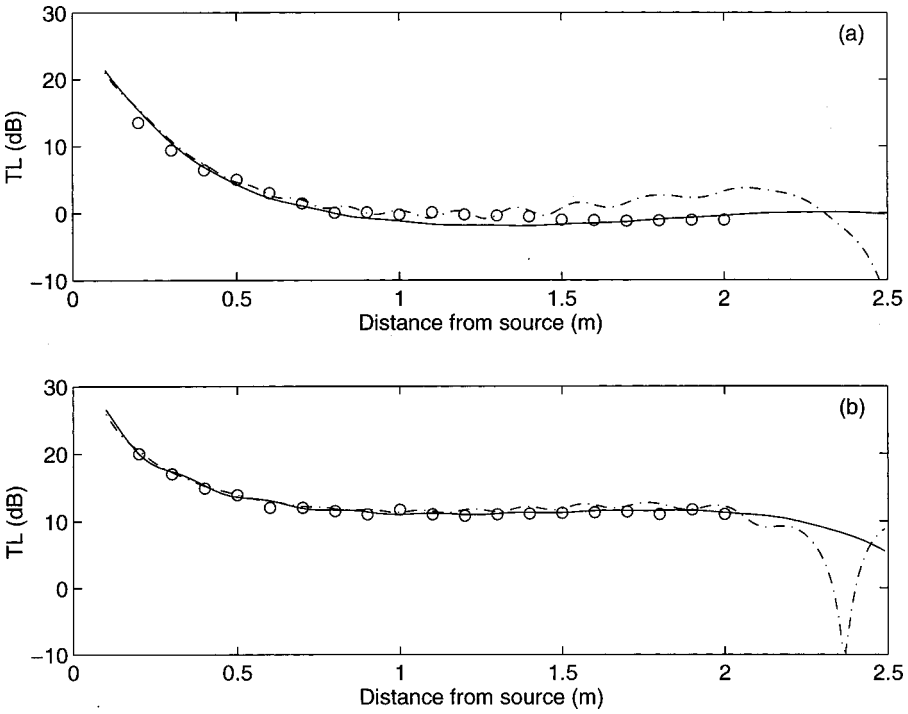

FIG. 5. Transmission loss due to a horizontal dipole source obtained at a frequency of 2915 Hz in a gradient with $R_c = 2.5$ m, over (a) a felt-covered concave surface with $z_s = z = 0.10$ m and (b) a rigid surface with $z_s = 0.02$ m and $z \sim 0.00$ m. Circles: measurements, solid curves: normal mode predictions for exponential profiles, dash-dotted curves: predictions for bilinear profiles.

kPa s m^{-2} and a rate of change of porosity with depth of 15 m^{-1} was found to be adequate in modeling the impedance of the felt-covered surface.

The hard and felt-covered surfaces allow sound propagation distances of up to 2.5 m in the direction perpendicular to the axis of the long cylinder. Propagation above the concave surface simulates propagation in the presence of a positive sound speed gradient with $R_c = 2.5$ m. The model was placed in an anechoic chamber which has an effective volume of $3 \times 3 \times 3$ m^3. A B&K 4311 1/4-in. condenser microphone was used to measure the sound pressure measurements. A Tannoy speaker type PD-30T, fitted with a tube of 3-cm internal diameter and 90 cm long, was used as the point monopole source. Two piezoceramic transducer discs with resonance frequencies of 2915 and 4350 Hz were found to be adequate as the dipole sources.[24] When the disc plane is vertical, it acts as a horizontal dipole source and, when it is horizontal, it acts as a vertical dipole source.

A PC-based maximum length sequence system analyzer (MLSSA) was used both as the signal generator for the sources and as the analyzer for subsequent signal processing. The impulse signal was analyzed using a half Blackman-Harris window and Fourier transformed.[25]

B. The sound field due to a monopole source over concave surfaces

The circles in Fig. 3(a) represent measurements for a frequency of 2915 Hz over the felt-covered concave surface. Both the source and receiver are at heights of 0.10 m. The solid curves represent predictions of the normal mode solution for the exponential profile and the dash-dotted curves represent predictions for the bilinear profile. The agreement between the measured data and the two curves is excellent out to 2.0 m (about 25 times the wave layer thickness, l_n) from the source. Beyond this distance, no reliable experimental data were obtained because the receiver is too close to the edge of the curved surface.

The circles in Fig. 3(b) represent measurements at 2915 Hz, with the receiver moved along the rigid surface ($z \sim 0.00$ m) and the source at a height of 0.02 m. Good agreement is found between measurements and predictions for the exponential profile (solid curves). However, there are considerable discrepancies between the measured data and the calculations for the bilinear profile (dash-dotted curves).

It is found that the predictions given by Eq. (7) for the exponential profiles agree with the experimental results obtained over the cylindrical concave surfaces. The agreement is better than that with the predictions given by Eq. (2) for the bilinear profiles. This accords with the general conclusion as with the propagation over cylindrical convex surfaces: the exponential sound speed profile is the most appropriate profile for the acoustic analogy.[3]

C. The sound field due to a horizontal dipole source over concave surfaces

The circles in Fig. 5(a) represent measurements at 2915 Hz over the felt-covered concave surface with both the source and receiver at heights of 0.10 m. The solid curves represent predictions for the normal mode solution from Eq. (18) for the exponential profile and the dash-dotted curves denote predictions for the normal mode solution from Eq. (15) for the bilinear profile. The agreement between the experimental data and the calculations for both profiles is very good out to 2.0 m (about 25 l_n) from the source.

In Fig. 5(b), we show experimental measurements (circles) at 2915 Hz, with the receiver moved along the rigid surface ($z \sim 0.00$ m) and the source height of 0.02 m. The calculations for the exponential profile are in excellent agreement with experimental data. However, there are consider-

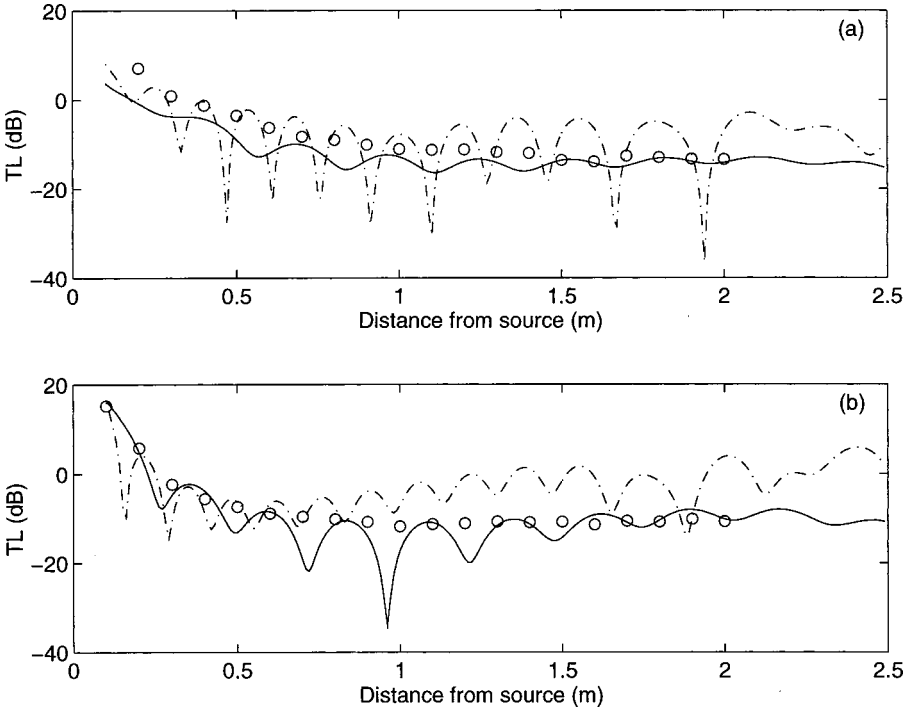

FIG. 6. Transmission loss due to a vertical dipole source at a frequency of 2915 Hz obtained in a gradient with $R_c = 2.5$ m, over (a) a felt-covered concave surface with $z_s = z = 0.10$ m and (b) a rigid surface with $z_s = 0.02$ m and $z \sim 0.00$ m. Circles: measurements, solid curves: normal mode predictions for exponential profiles, and dash-dotted curves: predictions for bilinear profiles.

able discrepancies between the measurements and the predictions for the bilinear profile (dash-dotted curves) at distances longer than 1.0 m from the source.

Comparing Figs. 3 and 5, it is noted that over concave surfaces, the sound field due to a horizontal dipole source is very similar to that due to a monopole source. This is consistent with what has been found in the case of convex surfaces.[7] Moreover, as was the case with a monopole source, the experimental measurements agree better with the predictions based on the exponential sound speed profile than those predicted according to the bilinear profile. Indeed, this should be the case because our mathematical analyses suggest that the conformal transformation of a cylindrical curve surface leads to the exponential rather than the bilinear sound speed profile.

D. The sound field due to a vertical dipole source over concave surfaces

The circles in Fig. 6(a) represent measurements at 2915 Hz over the felt-covered concave surface with both the source and receiver at heights of 0.10 m. The solid curves represent predictions from Eq. (19) for the exponential profile and the dash-dotted curves represent predictions from Eq. (16) for the bilinear profile. In contrast to the theoretical predictions, the experimental results lie on smooth curves (the dashed curves), which show similar trends to predictions of the monopole sound fields (cf. Fig. 3). Note that the scale in Fig. 6 is different from Figs. 3–5 in order to allow a better presentation of data.

Similar results have been obtained over the felt-covered concave surface. The circles in Fig. 6(b) represent data at 2915 Hz with the receiver moved along the rigid surface ($z \sim 0.00$ m) and the source at a height of 0.02 m.

It would appear that, for a vertical dipole source over a cylindrical concave surface, the agreement between the measurements and the normal mode predictions for both profiles is relatively poor. As mentioned earlier, the inaccuracy is due to the fact that the branch line contributions have been ignored in the normal mode solution. Nevertheless, relatively speaking, there is better agreement with the predictions based on the exponential profile than those based on the bilinear profile. It is of interest to note that, for the dipole source, use of the FFP predictions agrees reasonably well with experimental measurements (results are not shown for brevity).

IV. CONCLUSIONS

A normal mode solution has been developed for propagation in an exponential sound speed profile and used to predict the sound field diffracted by a cylindrical concave surface. Analytical expressions for dipole sources have been deduced directly from those for a monopole source.

A series of laboratory measurements of transmission loss have been conducted using a monopole source and horizontal or vertical dipole sources over cylindrical concave surfaces. The measurement results have been compared with normal mode predictions for both the exponential profile and the bilinear profile. For a monopole and a horizontal dipole, good agreement has been found between measurements and normal mode predictions using an exponential profile. However, the agreement is less satisfactory where the sound field was due to vertical dipole sources. The solution for a bilinear profile showed considerable disagreement with measurements in both monopole and horizontal dipole sound fields, and significant discrepancies from measurements in vertical dipole sound fields.

The predicted and measured transmission loss due to a horizontal dipole source, as a function of range, have been found to be close to those predicted for a monopole source.

However, the predicted transmission loss due to a vertical dipole source shows significant oscillations according to the normal mode solution.

ACKNOWLEDGMENTS

We thank the Open University Research Committee for financial support, Keith Attenborough for many useful discussions, and Shahram Taherzadeh for his latest version of the FFP. This work was supported in part by EPSRC Grant No. GR/L 15236. In the preparation of the revised manuscript, KML was partially supported by a Hong Kong Polytechnic University Research Grant, Project No. A-PB33.

[1] V. A. Fock, *Electromagnetic Diffraction and Propagation Problems* (Pergamon, Oxford, 1965).
[2] A. D. Pierce, *Acoustics: An Introduction to Its Physical Principles and Applications* (Acoustical Society of America, New York, 1989).
[3] A. Berry and G. A. Daigle, ''Controlled experiments of the diffraction of sound by a curved surface,'' J. Acoust. Soc. Am. **83**, 2047–2058 (1988) [see also A. Berry, ''Propagation of sound above a curved surface,'' J. Acoust. Soc. Am. Suppl. 1 **81**, S8 (1987)].
[4] Y. H. Berthelot and J. X. Zhou, ''Scale model experiments on the validity of the matched asymptotic expansions theory for sound diffraction by curved surfaces of finite impedance,'' J. Acoust. Soc. Am. **93**, 605–608 (1993).
[5] Y. H. Berthelot, ''A note on the acoustic penumbra behind a curved surface,'' J. Acoust. Soc. Am. **99**, 2428–2429 (1996).
[6] J. P. Chambers, R. Raspet, Y. H. Berthelot, and M. J. White, ''Use of the fast field program for predicting diffraction of sound by curved surfaces,'' J. Acoust. Soc. Am. **102**, 646–649 (1997).
[7] K. M. Li, Q. Wang, and K. Attenborough, ''Sound propagation over convex impedance surfaces,'' J. Acoust. Soc. Am. **104**, 2683–2691 (1998).
[8] M. Almgren, ''Simulation by using a curved ground scale model of outdoor sound propagation under the influence of a constant sound speed gradient,'' J. Sound Vib. **118**, 353–370 (1987).
[9] D. C. Pridmore-Brown and U. Ingard, ''Sound propagation into the shadow zone in a temperature-stratified atmosphere above a plane boundary,'' J. Acoust. Soc. Am. **27**, 36–42 (1955).
[10] D. C. Pridmore-Brown, ''Sound propagation in a temperature- and wind-stratified medium,'' J. Acoust. Soc. Am. **34**, 438–443 (1962).
[11] K. B. Rasmussen, ''Outdoor sound propagation under the influence of wind and temperature gradients,'' J. Sound Vib. **104**, 321–336 (1986).
[12] Y. Gabillet, H. Schroeder, G. A. Daigle, and A. L'Esperance, ''Application of the Gaussian beam approach to sound propagation in the atmosphere: Theory and experiments,'' J. Acoust. Soc. Am. **93**, 3105–3116 (1993).
[13] K. M. Li and Q. Wang, ''Analytical solutions for outdoor sound propagation in the presence of wind,'' J. Acoust. Soc. Am. **102**, 2040–2049 (1997).
[14] R. Raspet, G. Baird, and W. Wu, ''Normal mode solution for low-frequency sound propagation in a downward refracting atmosphere above a complex impedance plane,'' J. Acoust. Soc. Am. **91**, 1341–1352 (1992).
[15] A. D. Pierce and G. L. Main, in *Advances in Computer Methods for Partial Differential Equations 6*, edited by R. Vichnevetsky and R. Stepleman (IMACS, Rutgers Univ., New Brunswick, NJ, 1987), pp. 187–194.
[16] X. Di and K. E. Gilbert, ''The effect of turbulence and irregular terrain on outdoor sound propagation,'' in *Proceedings of 6th International Symposium on Long Range Sound Propagation* (1994), pp. 315–333.
[17] Q. Wang, ''Atmospheric refraction and propagation over curved surfaces,'' Ph.D. thesis, The Open University, UK, 1997.
[18] A. P. Dowling and J. E. Ffowcs Williams, *Sound and Sources of Sound* (Ellis Horwood, Chichester, 1983), p. 152.
[19] K. Attenborough, S. Taherzadeh, H. E. Bass, X. Di, R. Raspet, G. R. Becker, A. Gudesen, A. Chrestman, G. A. Daigle, A. L'Esperance, Y. Gabillet, K. E. Gilbert, Y. L. Li, M. J. White, P. Naz, J. M. Noble, and H. A. J. M. van Hoof, ''Benchmark cases for outdoor sound propagation models,'' J. Acoust. Soc. Am. **97**, 173–191 (1995).
[20] K. Attenborough, ''Ground parameter information for propagation modeling,'' J. Acoust. Soc. Am. **92**, 418–427 (1992).
[21] D. C. Strickler, ''Normal mode program with both discrete and branch line contributions,'' J. Acoust. Soc. Am. **61**, 856–861 (1974).
[22] S. N. Chandler-Wilde and D. C. Hothersall, ''Sound propagation above an inhomogeneous impedance plane,'' J. Sound Vib. **98**, 475–491 (1985).
[23] K. M. Li and Q. Wang, ''A BEM Approach to assess the acoustic performance of noise barriers in a refracting atmosphere,'' J. Sound Vib. **211**, 663–681 (1998).
[24] K. M. Li, S. Taherzadeh, and K. Attenborough, ''Sound propagation from a dipole source near an impedance plane,'' J. Acoust. Soc. Am. **101**, 3343–3352 (1997).
[25] D. D. Rife and J. Vanderkooy, ''Transfer-function measurement with Maximum-Length Sequences,'' J. Audio Eng. Soc. **37**, 419 (1989).